Controlling Mammalian Gene Expression by Allosteric Hepatitis Delta Virus Ribozymes

Yoko Nomura, Linlin Zhou, Anh Miu, and Yohei Yokobayashi*

Department of Biomedical Engineering, University of California, Davis, 451 Health Sciences Drive, Davis, California 95616, United States

S *Supporting Information*

ABSTRACT: We engineered small molecule responsive allosteric ribozymes based on the genomic hepatitis delta virus (HDV) ribozyme by replacing the P4-L4 stem-loop with an RNA aptamer through a connector stem. When embedded in the 3′ untranslated region of a reporter gene mRNA, these RNA devices enabled regulation of *cis*-gene expression by theophylline and guanine by up to 29.5-fold in mammalian cell culture. Furthermore, a NOR logic gate device was constructed by placing two engineered ribozymes in tandem, demonstrating the modularity of the RNA devices. The significant improvement in the regulatory dynamic range (ON/OFF ratio) of the RNA devices based on the HDV ribozyme should provide new opportunities for practical applications.

KEYWORDS: *ribozyme, HDV ribozyme, riboswitch, aptazyme, logic gate*
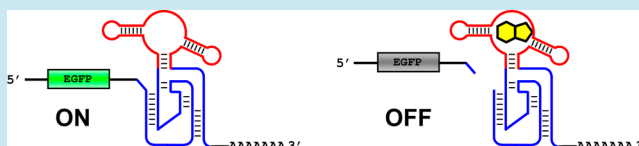
RNA devices designed to regulate gene expression in response to various chemical stimuli are a promising class of genetic devices for interfacing synthetic circuits with practical chemical information.[1−5] A widely adopted strategy to engineer RNA gene regulatory devices exploits a self-cleaving ribozyme fused to an RNA aptamer (i.e., aptazyme) that serves as a chemical sensor. With a suitable connection between the ribozyme and the aptamer, the ribozyme activity can be allosterically regulated by the aptamer ligand. These aptazymes can be integrated into various genetic and biological contexts to facilitate chemical gene regulation in *Escherichia coli*,[6,7] yeast,[8,9] and mammalian cells.[10−14]

However, the majority of the aptazymes that have been used to control gene expression in living cells have focused on a single class of self-cleaving ribozyme, namely, the hammerhead ribozyme. While the hammerhead ribozymes have been successfully exploited in many RNA devices, the regulatory dynamic ranges of these devices are often rather modest with up to 5- to 6-fold maximum change in gene expression in response to the ligand.

Hepatitis delta virus (HDV) ribozymes are an alternative class of self-cleaving ribozymes.[15] HDV ribozymes possess some distinct characteristics that may complement the widely used hammerhead ribozymes in engineering RNA devices for synthetic biology applications. For example, the HDV ribozyme structure has been found to be exceptionally stable, with in vitro activity reported in the presence of 5 M urea or 50% formamide or at 80 °C.[16−18] Although analogues of the HDV ribozyme have been recently discovered in diverse organisms,[15] the mammalian origin of the ribozyme provides confidence that the HDV ribozyme derivatives would be functional in mammalian cells.

Despite its long history of investigation, HDV ribozymes have not been extensively exploited for engineering applications except for *trans*-acting HDV ribozymes for targeted gene knockdown.[19] To our knowledge, only two allosteric HDV ribozymes characterized in vitro have been described in the literature. Kertsburg and Soukup described a theophylline-activated HDV ribozyme,[20] and Beaudoin and Perreault incorporated a G-quadruplex structure that regulates HDV ribozyme activity in response to potassium ion.[21]

Most recently, the Perreault group demonstrated the first chemically regulated HDV ribozymes embedded in the 5′ untranslated region (UTR) of mRNA in mammalian cell culture.[22] The chemical inputs used in this system, however, are 13- or 14-mer synthetic chemically modified oligonucleotides designed to hybridize with the complementary sequences strategically placed to modulate the ribozyme activity. Moreover, the dynamic ranges of gene expression (ON/OFF ratios) were modest, topping at about 2-fold.

We investigated the possibility of using HDV ribozymes as a platform for RNA devices for applications in mammalian cells. In this article, we report our engineering efforts of the first small molecule responsive HDV ribozymes that function in living cells. Our RNA devices exhibit excellent gene expression control in response to the two small molecules theophylline and guanine with ON/OFF ratios up to 29.5. Additionally, the modularity of the HDV aptazymes was highlighted by the integration of two aptazymes to construct a NOR logic gate device.

Rouleau et al. placed an active HDV ribozyme in the 5′ UTR of mammalian mRNA, but this resulted in only ∼40% reduction

in gene expression compared to its inactive mutant.[22] The authors speculate that their HDV ribozyme in the 5′ UTR may be acting as a translation initiator as recently shown in insect cells,[23] resulting in the rather modest ribozyme mediated gene regulation.

To achieve a higher dynamic range of gene regulation by the RNA devices, we first examined the effect of placing the wild-type genomic HDV ribozyme in the 3′ UTR of a reporter gene mRNA that has been shown to be effective with the hammerhead ribozyme.[11,13] Compared to the inactive mutant (Figure 1),[24] the wild-type HDV ribozyme reduced EGFP
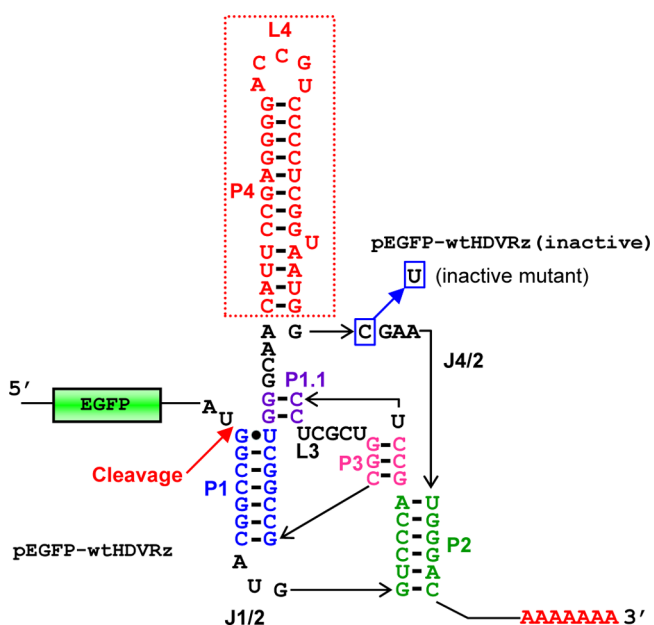

Figure 1. Schematic illustration of the EGFP reporter mRNA with the genomic HDV ribozyme embedded in the 3′ UTR. The secondary structure of the core HDV ribozyme motif is shown. The stem-loop P4-L4 is indicated in the dotted box, which was replaced with an appropriate aptamer in this work. The red arrow indicates the cleavage position. C-to-U point mutation to inactivate the ribozyme is shown in a blue box.

expression by approximately 90% when transfected into HEK 293 cells (Figure 2b). Insertion of the inactivated HDV ribozyme in the 3′ UTR resulted in approximately 23% decrease in gene expression relative to that of the parent vector ("empty vector") (Figures 2b and 3b). However, some of the aptazyme constructs exhibited higher expression levels (Figure 3b) comparable to that of the empty vector, indicating that this level of change in gene expression may be context-dependent and not intrinsic to the HDV ribozyme structure.

We then set out to explore the effects of replacing the stem-loop P4−L4 of the genomic HDV ribozyme with a small molecule binding RNA aptamer (Figure 1) because this position has been previously shown to yield a theophylline-responsive ribozyme in vitro.[20] We designed and constructed a small library of HDV-aptazyme mutants (Theo-lib1) in which four bases (two base pairs) connecting the theophylline aptamer[25] and the ribozyme were randomized (Figure 2a) in hope of generating aptazyme candidates with different connector stabilities. A total of 104 aptazyme mutant plasmids were individually purified, and each plasmid was transfected into HEK 293 cells in the presence (3 mM) and absence of theophylline. We identified one clone (Theo6HDV) that
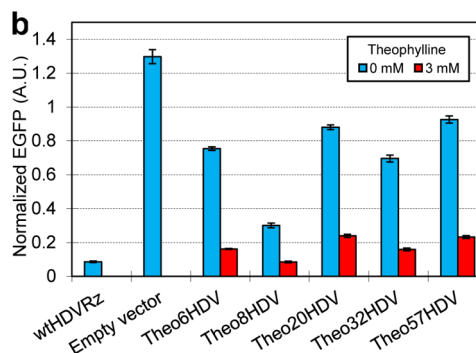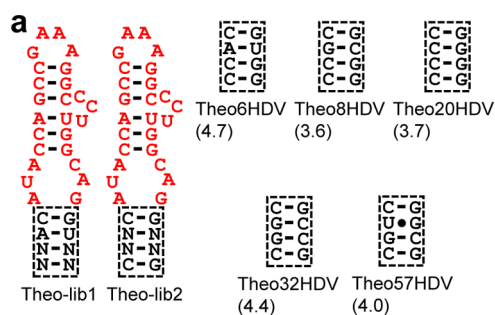

Figure 2. Theophylline-responsive HDV ribozymes. (a) Sequences of libraries Theo-lib1 and Theo-lib2 and the connector sequences discovered by screening. The numbers in the parentheses indicate the ON/OFF ratios of the aptazymes. (b) Expression levels of the EGFP-aptazyme constructs in the absence (blue) and presence (3 mM, red) of theophylline. EGFP expression is reported relative to the control with the inactive HDV ribozyme (1.0), after normalization for transfection efficiency using the cotransfected mCherry expression plasmid. The data shown are mean ± SD from four replicate samples.

exhibited an ON/OFF ratio of ∼4.7 (Figure 2b). Sequence examination of Theo6HDV revealed that the randomized bases formed two C-G pairs (Figure 2a). To further explore the sequence space, we screened a slightly different library (Theo-lib2) in which the base pair proximal to the ribozyme was fixed (C-G) to possibly stabilize the mutants and bias toward theophylline-responsive mutants (Figure 2a). We identified five switches from 100 mutants screened. Sequencing revealed that one was identical to Theo6HDV, and the other four all contained matching Watson−Crick or wobble (G·U) base pairs at the randomized positions, with the ON/OFF ratio ranging from 3.6 to 4.4 (Figure 2).

These results indicated that screening of a modest number of aptazyme mutants is a viable strategy for engineering mammalian RNA devices based on the HDV ribozyme. Although the throughput is limited by the time-consuming plasmid purification and transfection, careful library design can help identify functional switches from a small pool of aptazyme mutants.

This success with theophylline-responsive HDV aptazymes convinced us to attempt a similar search using guanine and its aptamer derived from the guanine riboswitch found in the 5′ UTR of *Bacillus subtilis xpt-pbuX* operon.[26] Recently, we have successfully engineered hammerhead aptazymes with the guanine aptamer.[13] After screening 100 mutants from the library shown in Figure 3a (Gua-lib), two excellent switches, Gua15HDV and Gua37HDV, were isolated that exhibit ON/OFF ratios of 11.0 and 8.6, respectively. Sequencing of the randomized bases again revealed Watson−Crick base pairs at these positions.
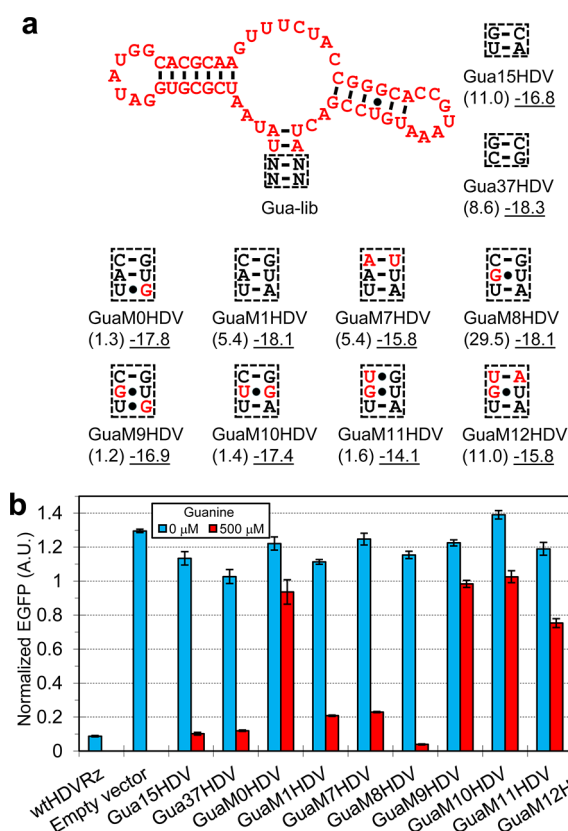
Figure 3. Guanine-responsive HDV ribozymes. (a) Sequences of library Gua-lib and the connector sequences discovered by screening (Gua15HDV and Gua37HDV) and iterative mutagenesis (GuaM[0/1/7/8/9/10/11/12]HDV). The numbers in the parentheses indicate the ON/OFF ratios of the aptazymes. The underlined numbers indicate the folding energy (ΔG, kcal/mol) of the connector-aptamer sequence flanked by one base each from the HDV ribozyme at the 5′ and 3′ ends as calculated by mfold.[27] (b) Expression levels of the EGFP-aptazyme constructs in the absence (blue) and presence (500 μM, red) of guanine. EGFP expression is reported relative to the control with the inactive HDV ribozyme (1.0), after normalization for transfection efficiency using the cotransfected mCherry expression plasmid. The data shown are mean $\pm$ SD from four replicate samples.

As an alternative strategy, we cloned and tested two connector sequences, M1 and M5, that were used in our recent hammerhead aptazymes.[13] Interestingly, M5, which yielded a functional switch when it was fused to the hammerhead, did not work when incorporated in the HDV ribozyme (data not shown). However, the M1 connector, which did not function in the context of the hammerhead ribozyme embedded in the 3′ UTR, afforded a respectable switch with an ON/OFF ratio of 5.4 (Figure 3). This result prompted us to examine several mutants that slightly modify the expected connector stem stability. First, we aimed to slightly weaken the stem by replacing each base pair by a weaker Watson−Crick or wobble base pair. GuaM0HDV has a single mutation that converts the U-A base pair closest to the ribozyme into a U·G wobble pair that largely abolishes the switch function (Figure 3). On the other hand, replacing the C-G base pair closer to the aptamer with a weaker A-U (GuaM7HDV) had no noticeable effect. However, a point mutation between these base pairs that introduced a wobble pair (GuaM8HDV) resulted in an exceptional switching performance with an ON/OFF ratio of 29.5 due to the lower

OFF level in the presence of guanine (Figure 3). Further weakening of a neighboring base pair resulted in a loss of switch function (GuaM9HDV, GuaM11), although one mutant GuaM12HDV retained the switching phenotype. Strikingly, flipping the G·U wobble pair in GuaM8HDV to U·G (GuaM10HDV) resulted in the loss of switch activity as well (Figure 3). The folding energies of the connector-aptamer sequences (Figure 3a) as calculated by mfold[27] did not show any apparent correlation with the switch performance (Supplementary Figure S1).

These results underscore the complexity of the aptazyme mechanisms beyond simple modulation of stem stability driven by the aptamer−ligand binding energy. Possibly, there may be sequence-dependent mechanisms that involve discrete structures whose relative abundances are influenced by aptamer−ligand interaction that may be difficult to accomplish by rational design.

We decided to further characterize the best aptazyme switch GuaM8HDV. Due to the low EGFP expression level in the presence of 500 μM guanine, the raw fluorescence signal obtained from these cells are close to the background cellular fluorescence of the untransfected cells, which may result in an increased experimental error. Consequently, we replaced EGFP with secreted embryonic alkaline phosphatase (SEAP), which produces a stronger fluorescence signal using a synthetic enzyme substrate to ensure more accurate quantification of the switch performance. Additionally, guanine concentration was varied to analyze the dose dependence of the switch. The result as indicated in Figure 4 shows that GuaM8HDV is mostly
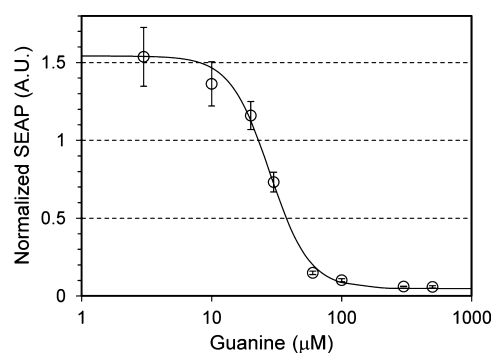

Figure 4. Detailed characterization of GuaM8HDV using SEAP as a reporter gene. The secreted SEAP levels of SEAP-GuaM8HDV were measured in different guanine concentrations from the cell culture medium and normalized for transfection efficiency using the cotransfected mCherry expression plasmid. The data shown are mean $\pm$ SD from four replicate samples. The curve is shown to guide the eye only.

repressed in the presence of 100 μM guanine. The ON/OFF ratio calculated at 0 and 500 μM guanine was 27.5, which is consistent with the analogous result obtained using EGFP (29.5).

These guanine-responsive HDV ribozymes and our recently reported guanine-responsive hammerhead ribozymes[13] suggest guanine as a useful chemical regulator of RNA devices in mammalian cell culture. As we reported previously, guanine exhibited no apparent cytotoxicity up to 500 μM, and our ribozymes are mostly activated at about 100 μM.[13] Moreover, the endogenous guanine level appears to have little or no detrimental effect on the ribozyme devices.

Next, we embedded two aptazymes that respond to theophylline (Theo6HDV) and guanine (GuaM8HDV) in tandem in the 3′ UTR of EGFP mRNA (Figure 5a). We
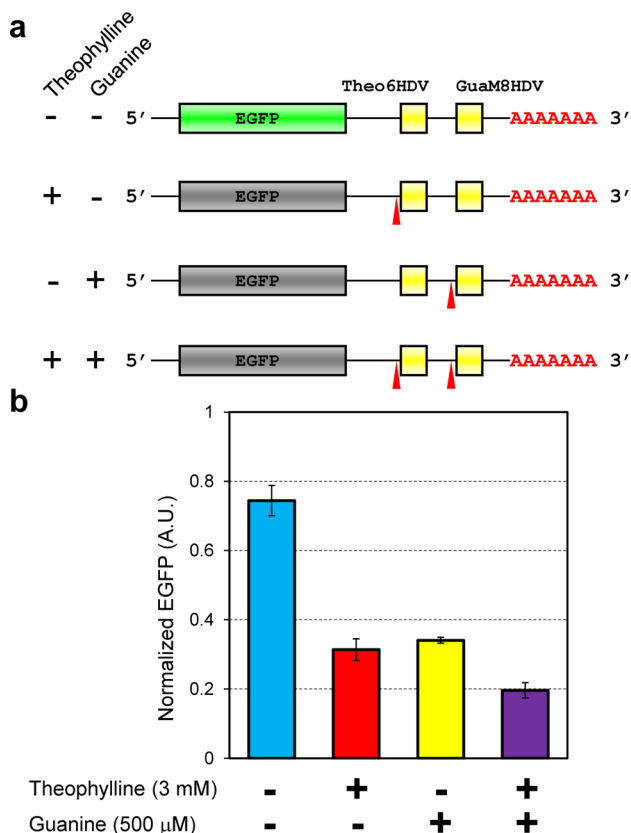

Figure 5. NOR logic gate device. (a) Schematic illustration of the NOR logic gate implemented by embedding Theo6HDV and GuaM8HDV aptazymes in tandem in the 3′ UTR of EGFP mRNA. Presence of theophylline and/or guanine results in ribozyme cleavage, which prevents EGFP expression. (b) Expression levels of the EGFP-Theo6HDV-GuaM8HDV device in the absence and presence of theophylline (3 mM) and/or guanine (500 μM). EGFP expression is reported relative to the control with the inactive HDV ribozyme (1.0), after normalization for transfection efficiency using the cotransfected mCherry expression plasmid. The data shown are mean ± SD from four replicate samples.

expected that the activation of either ribozyme by theophylline and/or guanine would result in diminished EGFP expression, therefore implementing a NOR logic gate. EGFP expression in response to the two chemical triggers confirmed the expected NOR logic response (Figure 5b). However, the OFF levels in the presence of theophylline and/or guanine were significantly higher compared to the results obtained with the single aptazyme constructs (Figure 2b and Figure 3b), perhaps due to folding interference between the two ribozymes. Nevertheless, this result supports the modularity of the HDV aptazyme devices as previously demonstrated for the hammerhead aptazymes.[28]

We reported a set of the first small molecule responsive allosteric HDV ribozymes that function in mammalian cells. The performance of the aptazymes as *cis*-acting gene switches is comparable, if not superior, to the similar devices based on the hammerhead ribozymes.[10,11,13] In particular, the aptazyme GuaM8HDV exhibited an excellent ON/OFF ratio approaching 30, which is a considerable improvement over the existing

RNA devices in mammalian cells. Chemically regulated ribozyme devices with more modest dynamic ranges have already been used to control cell proliferation[11] and for viral gene delivery.[29] Improved RNA devices with higher dynamic ranges such as those described in this report should facilitate similar and additional applications that require stringent gene regulation, for example, regulation of toxic or conditionally toxic genes.

We also note, however, that despite the unbiased nature of our screening method, we did not discover any aptazymes that are inhibited by the ligands (i.e., activate EGFP expression). This outcome probably reflects the biased distribution of the two switch phenotypes within the small sequence space represented by the plasmid libraries we could construct and screen and is by no means indicative of the intrinsic limitations of the HDV ribozyme motif. To enhance the chances to obtain improved or different switch phenotypes, it may be necessary to either increase the throughput to widen the explored sequence space or rationally design a library to predispose the mutants to adopt specific mechanisms. Increasing screening throughput, especially using mammalian cells, may require the use of new experimental tools such as cell sorting or high-throughput sequencing, while guided library design would likely require additional biochemical and structural insights into the HDV ribozyme. Additionally, the recent discovery of a large number of HDV ribozyme analogues across organisms aided by computational tools[15,30] dramatically increases the repertoire of the potential ribozyme scaffolds on which to engineer novel functions. Taken together, we believe HDV ribozymes and their analogues are attractive resources for engineering novel RNA devices.

■ METHODS

Library and Plasmid Construction. All plasmids were prepared by standard recombinant DNA techniques. Plasmids encoding the *cis*-acting (3′ UTR) HDV aptazymes were derived from pEGFP-N1 (Clontech). Appropriate aptazyme sequences were cloned in the 3′ UTR of the EGFP transcript. All plasmids were purified using Zyppy Plasmid Miniprep kit (Zymo Research). Nucleotide sequences of the plasmids are provided in Supporting Information.

Cell Culture and Transfection. HEK293 cells were maintained in a 5% CO_2 humidified incubator at 37 °C in Dulbecco's modified Eagle's medium (DMEM) (Mediatech) supplemented with 10% fetal bovine serum (FBS) (Gibco) and 1× antibiotic-antimycotic (Gibco). One day before transfection, HEK293 cells were trypsinized and diluted appropriately with fresh complete medium, and 2.4×10^4 cells/well (~100 μL) were seeded onto 96-well plates. Fifty nanograms of an EGFP/SEAP-aptazyme plasmid or an appropriate control plasmid and 10 ng of pCMV-mCherry plasmid (constitutively expresses mCherry) were cotransfected using 1 μL of PolyFect reagent (QIAGEN) per well according to the manufacturer's instruction. After 3.5 h of incubation, the medium was removed and replaced with 100 μL of fresh complete medium containing appropriate concentrations of theophylline or guanine. Guanine (Acros) was first dissolved in 100× concentrations in 0.2 M NaOH and was diluted 100-fold with the complete medium immediately before use. The cells were incubated for additional 18 h before EGFP or SEAP assay.

EGFP Assay. Cellular fluorescence was measured and normalized according to our previous report.[12] Briefly, the cell culture medium was replaced with phosphate buffered

saline (PBS) (150 μL per well) and incubated at 37 °C until measurement. Fluorescence intensities were measured for EGFP (484 nm excitation/510 emission/5 nm bandwidth) and mCherry (587 nm excitation/610 nm emission/10 nm bandwidth) using Safire2 microplate reader (Tecan). The raw fluorescence values were first subtracted with that of the untransfected cells (background). For each well, EGFP fluorescence was normalized by mCherry ([EGFP fluorescence]/[mCherry fluorescence]) to account for variations in transfection efficiency. The values were further normalized by the cells transfected with pEGFP-wtHDVRz(inactive)/pCMV-mCherry (= 1.0). The reported values are mean ± SD from four replicate samples.

SEAP Assay. Approximately 100 μL of the medium from each well containing the secreted SEAP was sampled and centrifuged in a 1.5 mL microcentrifuge tube. Supernatant (80 μL) from each well was transferred to a fresh tube and stored at −20 °C until SEAP assay. After removing the remaining medium, PBS (150 μL) was added to each well, and the cells were incubated at 37 °C until mCherry fluorescence was measured as described above. SEAP assay of the medium was performed using Great EscAPe SEAP Fluorescence Detection Kit (Clontech) according to the manufacturer's instructions. The samples were diluted 16-fold before measurement after confirming that the SEAP activities fall within the linear range of the assay. Fluorescence of the SEAP-cleaved substrate was measured (360 nm excitation/449 nm emission/20 nm bandwidth) using a Safire2 microplate reader. The values were normalized by mCherry fluorescence after subtracting the background values obtained using untransfected cells.

■ ASSOCIATED CONTENT

ⓢ Supporting Information
Sequence information of the plasmids described and a supporting figure. This material is available free of charge via the Internet at http://pubs.acs.org.

■ AUTHOR INFORMATION

Corresponding Author
*Tel: +1-530-754-9676. Fax: +1-530-754-5739. E-mail: yoko@ucdavis.edu.

Notes
The authors declare no competing financial interest.

■ ACKNOWLEDGMENTS

■ REFERENCES

(1) Isaacs, F. J., Dwyer, D. J., and Collins, J. J. (2006) RNA synthetic biology. *Nat. Biotechnol. 24*, 545−554.
(2) Liang, J. C., Bloom, R. J., and Smolke, C. D. (2011) Engineering biological systems with synthetic RNA molecules. *Mol. Cell 43*, 915−926.
(3) Saito, H., and Inoue, T. (2009) Synthetic biology with RNA motifs. *Int. J. Biochem. Cell Biol. 41*, 398−404.
(4) Weigand, J. E., and Suess, B. (2009) Aptamers and riboswitches: perspectives in biotechnology. *Appl. Microbiol. Biotechnol. 85*, 229−236.
(5) Wieland, M., and Fussenegger, M. (2010) Ligand-dependent regulatory RNA parts for Synthetic Biology in eukaryotes. *Curr. Opin. Biotechnol. 21*, 760−765.
(6) Ogawa, A., and Maeda, M. (2008) An artificial aptazyme-based riboswitch and its cascading system in E. coli. *ChemBioChem 9*, 206−209.
(7) Wieland, M., and Hartig, J. S. (2008) Improved aptazyme design and in vivo screening enable riboswitching in bacteria. *Angew. Chem., Int. Ed. 47*, 2604−2607.
(8) Wittmann, A., and Suess, B. (2011) Selection of tetracycline inducible self-cleaving ribozymes as synthetic devices for gene regulation in yeast. *Mol. Biosyst. 7*, 2419−2427.
(9) Win, M. N., and Smolke, C. D. (2007) A modular and extensible RNA-based gene-regulatory platform for engineering cellular function. *Proc. Natl. Acad. Sci. U.S.A. 104*, 14283−14288.
(10) Ausländer, S., Ketzer, P., and Hartig, J. S. (2010) A ligand-dependent hammerhead ribozyme switch for controlling mammalian gene expression. *Mol. Biosyst. 6*, 807−814.
(11) Chen, Y. Y., Jensen, M. C., and Smolke, C. D. (2010) Genetic control of mammalian T-cell proliferation with synthetic RNA regulatory systems. *Proc. Natl. Acad. Sci. U.S.A. 107*, 8531−8536.
(12) Kumar, D., An, C. I., and Yokobayashi, Y. (2009) Conditional RNA interference mediated by allosteric ribozyme. *J. Am. Chem. Soc. 131*, 13906−13907.
(13) Nomura, Y., Kumar, D., and Yokobayashi, Y. (2012) Synthetic mammalian riboswitches based on guanine aptazyme. *Chem. Commun. (Cambridge) 48*, 7215−7217.
(14) Wieland, M., Auslander, D., and Fussenegger, M. (2012) Engineering of ribozyme-based riboswitches for mammalian cells. *Methods 56*, 351−357.
(15) Webb, C. H., and Lupták, A. (2011) HDV-like self-cleaving ribozymes. *RNA Biol. 8*, 719−727.
(16) Perrotta, A. T., Shih, I., and Been, M. D. (1999) Imidazole rescue of a cytosine mutation in a self-cleaving ribozyme. *Science 286*, 123−126.
(17) Rosenstein, S. P., and Been, M. D. (1990) Self-cleavage of hepatitis delta virus genomic strand RNA is enhanced under partially denaturing conditions. *Biochemistry 29*, 8011−8016.
(18) Wu, H. N., and Lai, M. M. (1990) RNA conformational requirements of self-cleavage of hepatitis delta virus RNA. *Mol. Cell. Biol. 10*, 5575−5579.
(19) Asif-Ullah, M., Lévesque, M., Robichaud, G., and Perreault, J. P. (2007) Development of ribozyme-based gene-inactivations; the example of the hepatitis delta virus ribozyme. *Curr. Gene Ther. 7*, 205−216.
(20) Kertsburg, A., and Soukup, G. A. (2002) A versatile communication module for controlling RNA folding and catalysis. *Nucleic Acids Res. 30*, 4599−4606.
(21) Beaudoin, J. D., and Perreault, J. P. (2008) Potassium ions modulate a G-quadruplex-ribozyme's activity. *RNA 14*, 1018−1025.
(22) Rouleau, S. G., Jodoin, R., Bisaillon, M., and Perreault, J. P. (2012) Programming a highly structured ribozyme into complex allostery using RNA oligonucleotides. *ACS Chem. Biol. 7*, 1802−1806.
(23) Ruminski, D. J., Webb, C. H., Riccitelli, N. J., and Lupták, A. (2011) Processing and translation initiation of non-long terminal repeat retrotransposons by hepatitis delta virus (HDV)-like self-cleaving ribozymes. *J. Biol. Chem. 286*, 41286−41295.
(24) Kumar, P. K. R., Suh, Y. A., Miyashiro, H., Nishikawa, F., Kawakami, J., Taira, K., and Nishikawa, S. (1992) Random mutations to evaluate the role of bases at two important single-stranded regions of genomic HDV ribozyme. *Nucleic Acids Res. 20*, 3919−3924.
(25) Jenison, R. D., Gill, S. C., Pardi, A., and Polisky, B. (1994) High-resolution molecular discrimination by RNA. *Science 263*, 1425−1429.
(26) Mandal, M., Boese, B., Barrick, J. E., Winkler, W. C., and Breaker, R. R. (2003) Riboswitches control fundamental biochemical pathways in Bacillus subtilis and other bacteria. *Cell 113*, 577−586.
(27) Zuker, M. (2003) Mfold web server for nucleic acid folding and hybridization prediction. *Nucleic Acids Res. 31*, 3406−3415.
(28) Win, M. N., and Smolke, C. D. (2008) Higher-order cellular information processing with synthetic RNA devices. *Science 322*, 456−460.

(29) Ketzer, P., Haas, S. F., Engelhardt, S., Hartig, J. S., and Nettelbeck, D. M. (2012) Synthetic riboswitches for external regulation of genes transferred by replication-deficient and oncolytic adenoviruses. *Nucleic Acids Res. 40*, e167.

(30) Webb, C. H., Riccitelli, N. J., Ruminski, D. J., and Lupták, A. (2009) Widespread occurrence of self-cleaving ribozymes. *Science 326*, 953.